

Fig. S1. Expression patterns of CYP77A4 gene from a publicly available database.
 (A and B) Expression levels of *CYP77A4* gene in various tissues (A) and embryos (B) based on microarray data taken from the eFP-browser (<http://bar.utoronto.ca/efp/cgi-bin/efpWeb.cgi>) (Winter *et al.*, 2007). Red indicates a relatively higher expression level.

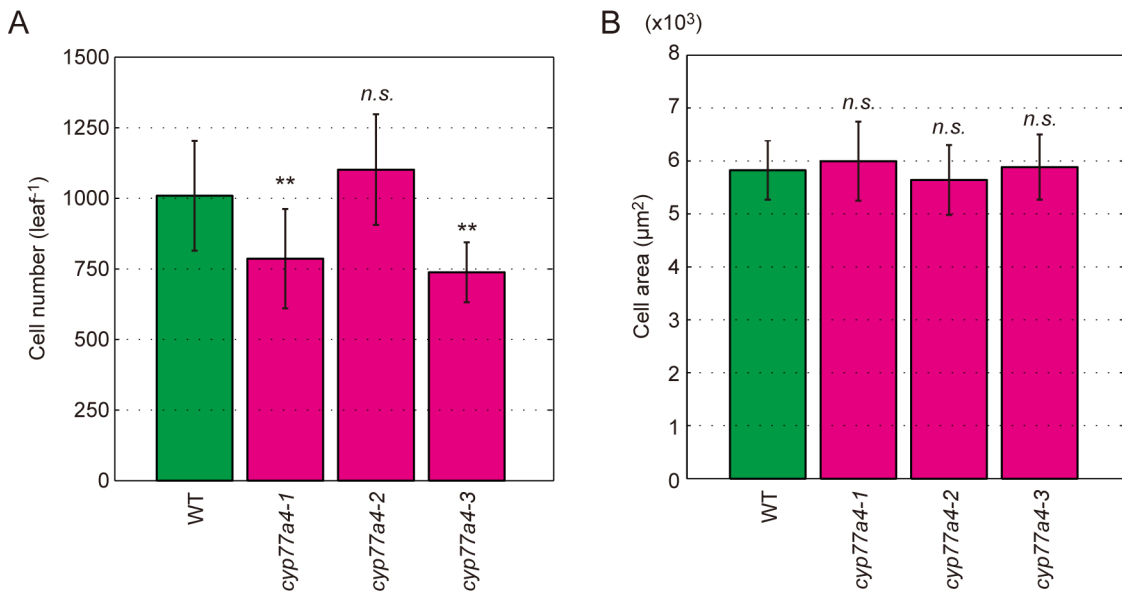


Fig. S2. Palisade cell number and size in WT and *cyp77a4* cotyledons.

(A and B) Cotyledons from 21-day-old plants were collected, fixed, and cleared for microscopic investigations. The numbers (A) and areas (B) of palisade cells in the WT and *cyp77a4* mutants. The mean \pm s.d. is shown for each line ($n = 12$ for WT, $n = 77$ for *cyp77a4-1*, $n = 69$ for *cyp77a4-2*, and $n = 68$ for *cyp77a4-3*). ** $P < 0.01$ compared with the WT (Student's *t*-test). n.s., non significant ($P > 0.05$ with Student's *t*-test).

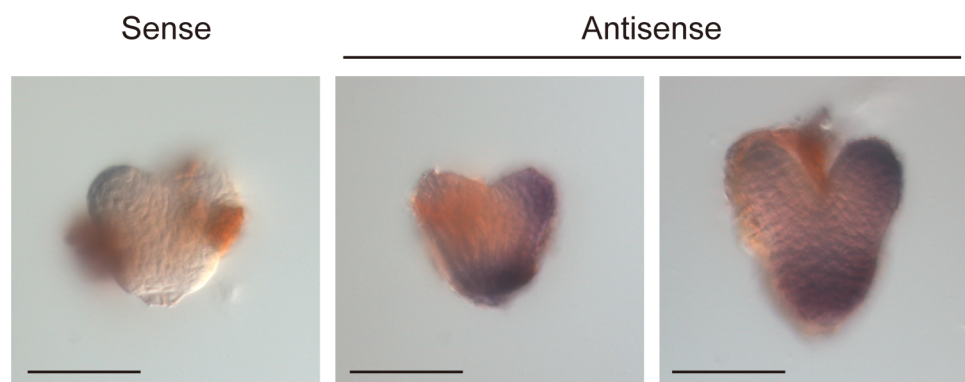


Fig. S3. Expression analysis of *CYP77A4* by whole mount *in situ* hybridization.

Accumulation of *CYP77A4* transcripts in embryos. Probe to the sense strand of the *CYP77A4* transcript was used as a negative control. Whole mount *in situ* hybridization was performed as follows: *CYP77A4* cDNA was cloned into pZErO-2 vector (Thermo Fisher Scientific) using primers listed below. DIG-labeled RNA probes of both sense and antisense strands were transcribed by DIG RNA Labeling Kit (Roche). The embryos were dissected from 5-week-old plants and fixed in a fixative containing 4% (w/v) paraformaldehyde and 1% (v/v) glutaraldehyde in PBS. The subsequent procedures were described elsewhere (Rozier *et al.*, 2014). Scale bars: 50 µm.

(Primers used)

5'-CTGCTTGAGTCAACAAGAAATAAACAG-3'

5'-AGCAAACACACCTTACAATAATCTC-3'

(Reference)

Rozier, F., Mirabet, V., Vernoux, T. and Das, P. (2014). Analysis of 3D gene expression patterns in plants using whole-mount RNA *in situ* hybridization. *Nat. Protoc.* **9(10)**, 2464-2475.

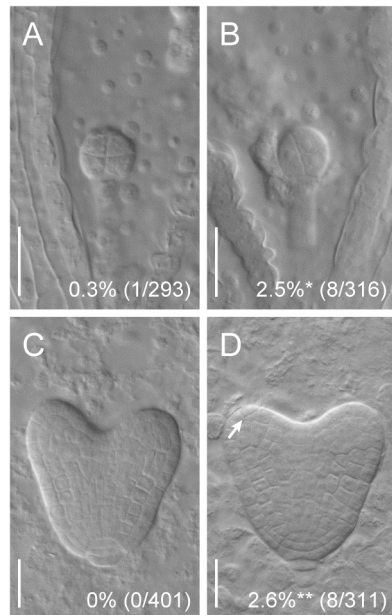


Fig. S4. Irregular cell division pattern in the *cyp77a4* mutants.

(A-D) Embryos at the earlier development stage than 32-cell and at the heart stages in the WT (A and C) and the *cyp77a4-3* mutants (B and D). Penetrance of the irregular cell division pattern (A and B) and periclinal/oblique cell division in the protodermal tissue (C and D) were calculated as a frequency of the embryos with altered division pattern against normal embryos. An arrow indicates the irregular cell division. * $P<0.05$, ** $P<0.01$ compared with the corresponding WT (two-tailed Fisher's exact test). Differential interference contrast images of cleared immature seeds are shown. Samples were collected from 5-week-old plants. Scale bars: 25 μ m.

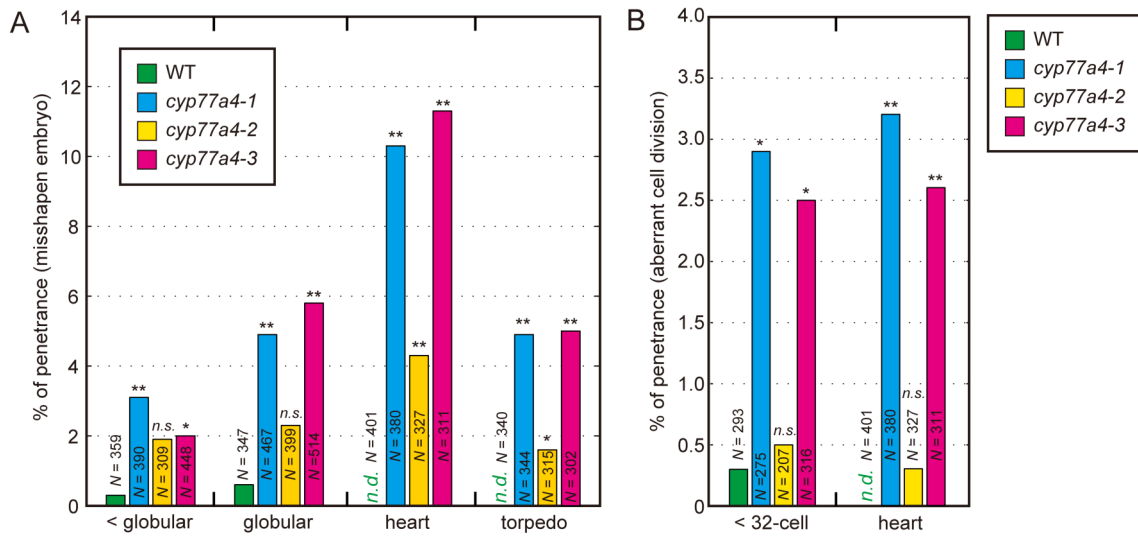


Fig. S5. Penetrance of abnormal morphology and aberrant cell division in *cyp77a4* embryos.

(A and B) Missshapen embryos at the earlier development stage than globular (< globular), globular, heart and torpedo stages (A), and irregular divisions at the earlier development stage than 32-cell (< 32-cell) and heart stages (B) were observed in *cyp77a4* mutants, particularly in the null alleles (*cyp77a4-1* and *cyp77a4-3*), when compared with the WT controls. * $P<0.05$, ** $P<0.01$ compared with the corresponding WT at each developmental stage (two-tailed Fisher's exact test). n.s., non significant ($P>0.05$). n.d., non detected.

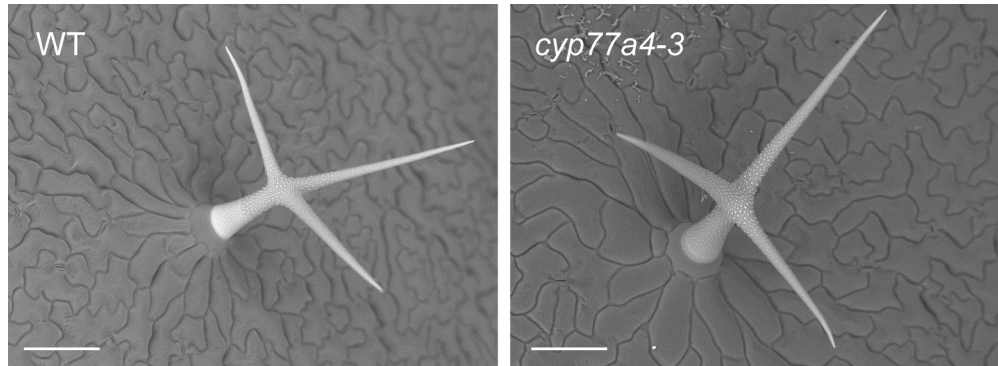


Fig. S6. Scanning electron microscopy images of trichomes.

Mature leaves of 4-week-old WT and *cyp77a4-3* plants were sampled. Scanning electron microscopy (SEM) was performed using a Hitachi TM3000 SEM microscope at 15 kV. Scale bars: 100 μ m.

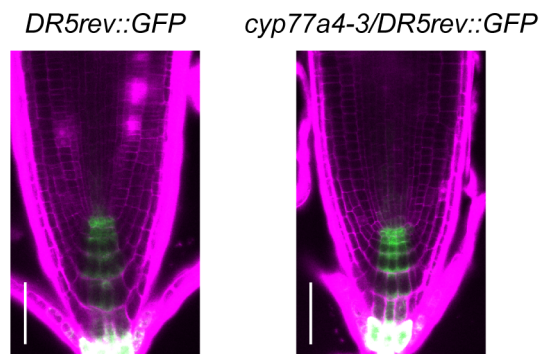


Fig. S7. Expression of *DR5_{rev}::GFP* in WT and *cyp77a4* roots.

Confocal images of the root tip in 7-day-old seedlings in *DR5_{rev}::GFP* and *cyp77a4-3/DR5_{rev}::GFP*. GFP fluorescence and propidium iodide stain are shown in green and magenta, respectively. Scale bars: 50 μ m.

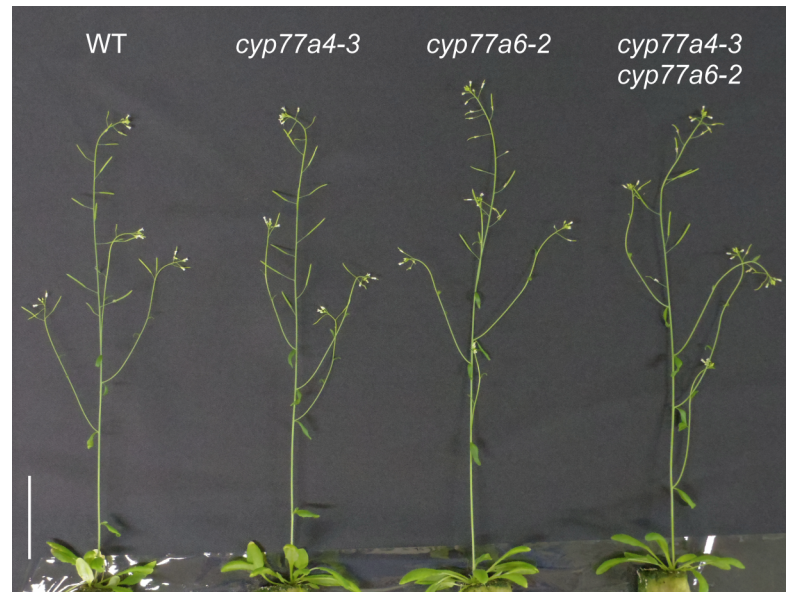


Fig. S8. Overall growth of the *cyp77a4* *cyp77a6* double mutant.

Four-week-old WT, *cyp77a4-3*, *cyp77a4-2*, and *cyp77a4-3 cyp77a6-2* plants. Scale bar: 5 cm.

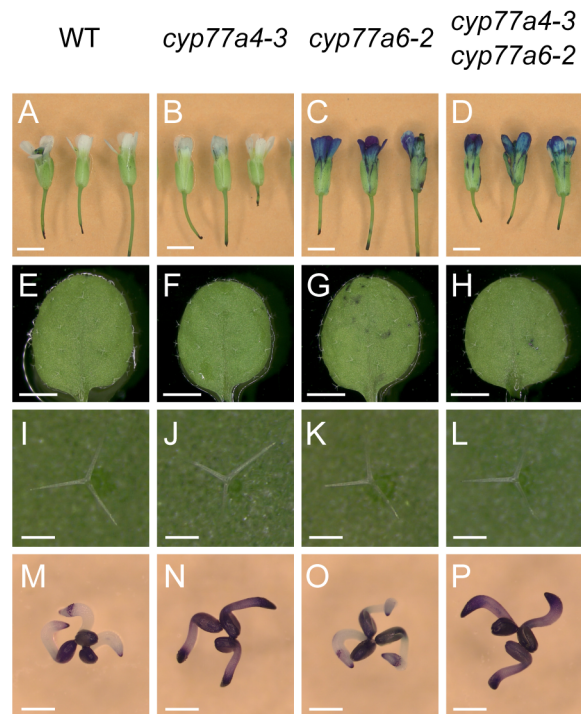


Fig. S9. Toluidine blue permeability of the *cyp77a4* mutant.

(A–P) Flowers (A–D), leaves (E–H), trichomes (I–L), and germinating embryos (M–P) of the WT (A,E,I,M), *cyp77a4-3* (B, F, J, N), *cyp77a6-2* (C, G, K, O), and *cyp77a4-3 cyp77a6-2* (D,H,L,P) stained by toluidine blue. Scale bars: 2 mm (A–H), 200 μ m (I–L) and 500 μ m (M–P).

Table S1. Arabidopsis T-DNA insertion mutants of cytochrome P450 genes

Stock number	Locus	Gene name	Genotyping primers	
			Forward 5'-3'	Reverse 5'-3'
SALK_001709C	At3g48520	CYP94B3	TGCTCAATCCAATTGGTTTC	AAAACGAAGCGTGTGTTGAAC
SALK_003101C	At3g30290	CYP702A8	TCCCTCATATAATCATGCAACG	AACTCTCCAAACTCCTCTCCG
SALK_005826C	At4g00360	CYP86A2	ATCGAACACATGCTCAAGACC	GAATTCCAAGCAATCCTCTCC
SALK_006594C	At3g20110	CYP705A20	AGCAATGTTGACCGTTGACTC	ACGTTACGGTTGTTGATGAGC
SALK_008736C	At3g48290	CYP71A24	TCGGCATAACGTAACGTTTC	GCTCTTCTTCCCTCTCGACTG
SALK_009366C	At3g53300	CYP71B31	TCCAACGTTAGGATCACGTC	ATGCTCAAACACAAACCTTGG
SALK_011806C	At1g16410	CYP79F1	CTAGGTCCAATATTCCGCC	CACAAGCCTGTCTTCCAAC
SALK_012075C	At1g13110	CYP71B7	TCAGAGCCAACCAAACAAAG	GAGGAAGCTTCCATTTGAGG
SALK_019080C	At3g10570	CYP77A6	GCTCAATGAAAGTCCAGCATC	GCTCCGTTTATTCCAAGGAG
SALK_021290C	At2g46960	CYP709B1	GTCAGGTGCCTGAAACTTG	TGAGATGCATATCCTGGCTC
SALK_023343C	At3g26280	CYP71B4	CAGAAGGCATGGTAGTCGAAG	TCCGATGTCTTACCGTTACG
SALK_023674C	At3g53290	CYP71B30P	CTCCCTCTAAACCAAACCGAC	TCCCAAGATTAACAATGTCCG
SALK_036476C	At3g13730	CYP90D1	TTTGCCTTGTGAAGGAATACG	GAAGGAATTGACAGGGAGAGCC
SALK_046395C	At5g04660	CYP77A4	TGTTTACAAAGCAATGAGGGC	TGCGAATCCTGAGATTCAATC
SALK_047258C	At3g14610	CYP72A7	CCCAACTCTGCTGAAACAAAG	TTCCCTTGCATTAGATCATC
SALK_048981C	At4g15110	CYP97B3	CCTGGAGCTCTAACATCTG	ATATTGGACAATGCGAGCAAC
SALK_056876C	At2g45580	CYP76C3	CACAAACACAGTGGTTACCTG	GTACGGCACAAAGAGATTGG

Stock number	Locus	Gene name	Genotyping primers	
			Forward 5'-3'	Reverse 5'-3'
SALK_057638C	At3g53280	CYP71B5	CGATCTTGAGACTTGTAGCCG	ATGGTGTCTTGGAATGCTG
SALK_081643C	At3g01900	CYP94B2	CCACTATGCGTCTGGTCTCTC	CACCCAAACTTCATCTCATTG
SALK_086471C	At3g26330	CYP71B37	TTTGCCACTACACTCATTCTC	CCTGATGGGTTGAATCAAATG
SALK_087617C	At1g13090	CYP71B28	CTGAAGATCCACTCGATGAGC	ACACC GTGAAGATTGTTGC
SALK_090621C	At4g15330	CYP705A1	CCCATTTTATGATCAATGGG	GTGCCGA ACTGTATACGCATG
SALK_090743C	At3g44970	CYP708A4	TAGTTTAGTGGTTGCAGGG	TATTGCCGTGTTGAGGAAGTC
SALK_092654C	At1g79370	CYP79C1	CGGAGACGAAGAACATGATGTC	TAACCGGTATGATCAAGCTGG
SALK_094765C	At1g64950	CYP89A5	GAGTAGCAGAACTCACCAAAACC	AGGC GAAAGAAGAGGGAGATTG
SALK_096641C	At1g13080	CYP71B2	CACAGGAGATTGCTTCAAAGC	TAAAGGCATAATCATTGCCG
SALK_109844C	At1g13070	CYP71B27	CACAGGAGATTGCTTCAAAGC	CTCTATCGGCAATCCTCACAG
SALK_113348C	At4g39950	CYP79B2	CCCATATCGGCTAAGAAGGAC	AAGTTGTGATGACGGAACTCG
SALK_114536C	At2g46660	CYP78A6	CCGGTTAAAGAACATGGCTTAC	AACTCCAAGGATCAACCCAC
SALK_120416C	At1g17060	CYP72C1	CCGACATGTGAAGTAAGCTGG	AACAGAAAAAGCCAAAAGGC
SALK_129352C	At3g30180	CYP85A2	CCATGGGTTAAAGATCATTGG	TTGTTGTGGGAACTCTATCGG
SALK_130811C	At3g14630	CYP72A9	GCATTCTCAATTCAAAACATGG	TCCTGCATACCGTAAGAAC
SALK_142442C	At2g42250	CYP712A1	TCCATCTATTGGATTCAAGGG	CTCTGCAGAACCAAACCTCAGG
SALK_149325C	At4g15440	CYP74B2	CAACAGCTTAATTGAACCGG	ACATTTCTGGGAACAATCG
SALK_150522C	At1g74550	CYP98A9	GTCAGAGCTCGAGACCACAAC	GTCGCACAAGTAGTAGGTGCC

Table S2. Frequencies of cotyledon phenotypes in two *cyp77a6* alleles

Genotype	Frequencies of cotyledon number (%)				Total number
	One	Two (Irregular)	Two (Normal)	Three	
WT	0	0	100.0	0	964
<i>cyp77a6-1</i>	0	0	100.0	0	949
<i>cyp77a6-2</i>	0	0	100.0	0	940

The unseparated cotyledon (Fig. 2D) and cup-shaped cotyledon (Fig. 2F) were counted as One in addition to the single cotyledon (Fig. 2E). Two separated cotyledons with bilateral asymmetry around the shoot apical meristem (Fig. 2C) were counted as Two (Irregular).

Table S3. Frequencies of cotyledon phenotypes in the *cyp77a4 cyp77a6* double mutant

Genotype	Frequencies of cotyledon number (%)				Total number
	One	Two (Irregular)	Two (Normal)	Three	
WT	0	0	99.9	0.1	932
<i>cyp77a4-3</i>	1.0	0.6	98.4	0	945
<i>cyp77a6-2</i>	0	0	99.9	0.1	971
<i>cyp77a4-3 cyp77a6-2</i>	1.4	0.7	97.8	0	967

The unseparated cotyledon (Fig. 2D) and cup-shaped cotyledon (Fig. 2F) were counted as One in addition to the single cotyledon (Fig. 2E). Two separated cotyledons with bilateral asymmetry around the shoot apical meristem (Fig. 2C) were counted as Two (Irregular).

Table S4. Primers used for genotyping, RT-PCR, qRT-PCR and vector constructions.

#	Primer name	Sequence 5'-3'
T-DNA genotyping		
1	<i>cyp77a4-1_LP_SALK_046395</i>	TGTTTACAAAGGAATGAGGGC
2	<i>cyp77a4-1_RP_SALK_046395</i>	TGCGAATCCTGAGATTCAATC
3	<i>cyp77a4-2_LP_SALK_112368</i>	GAATATCGTAACCAGCAAGCG
4	<i>cyp77a4-2_RP_SALK_112368</i>	AACGTATGGCCCGATTTTAC
5	<i>cyp77a4-3_LP_SALK_076143</i>	TGGGACACTCCTGTTAAAGC
6	<i>cyp77a4-3_RP_SALK_076143</i>	GTTTCCCGAATTCTTGAGAC
7	<i>cyp77a6-1_LP_SALK_019080</i>	GCTCAATGAAAGTCCAGCATC
8	<i>cyp77a6-1_RP_SALK_019080</i>	GCTCCGTTTATTCCAAGGAG
9	<i>cyp77a6-2_LP_SALK_023926</i>	AAATCAATTCACTTCCGGCG
10	<i>cyp77a6-2_RP_SALK_023926</i>	CTTCACCGTTAACGCTTCAG
Semiquantitative RT-PCR and qRT-PCR		
11	<i>CYP77A4_RT-PCR_Fwd</i>	GAATCCGACCCGAACAATCTT
12	<i>CYP77A4_RT-PCR_Rev</i>	TCCGCGCAAGCATCAAAT
13	<i>ACTIN2_RT-PCR_Fwd</i>	TTCCTCTCCGCTTGAATTGTCTCG
14	<i>ACTIN2_RT-PCR_Rev</i>	GGATGGCATGAGGAAGAGAGAAACC
15	<i>CYP77A4_qRT-PCR_Fwd</i>	TGACGCATGCCGTTATGG
16	<i>CYP77A4_qRT-PCR_Rev</i>	TCCGCGCAAGCATCAAAT
Vector construction		
17	<i>At5g04650_Intron1_Fwd</i>	caccGTGTTAAGAAATGAGTTGGTGGTT
18	<i>CYP77A4_CDS_Fwd</i>	caccATGTTCCCTAACTCCTTTCTCC
19	<i>CYP77A4_5'-UTR_Rev</i>	TTTAGCTCTGTTATTCTGTGACTC
20	<i>CYP77A4_CDS_Rev</i>	CTAAATCCTGGTTGACCATAGCT
21	<i>CYP77A4_CDS_Rev (-TAG)</i>	AATCCTGGTTGACCATAGCTCT
22	<i>CYP77A4_3'-UTR_Rev</i>	GTGTAGATTGGTACTTAATGTTATAA